https://doi.org/10.5194/egusphere-2026-2068
Preprint. Discussion started: 21 April 2026

Surface charging of the JUICE spacecraft during the 2024 Earth gravity assist

Maryam Zeroual[1,2], Mika K. G. Holmberg[1], Francois Gutierrez[3], Fredrik L. Johansson[3], Jan-Erik Wahlund[4], Markus Fräenz[5], Pierre Henri[6,7], Xavier Vallieres[6], and Alexandra R. Fogg[1]

[1]Astronomy & Astrophysics Section, School of Cosmic Physics, Dublin Institute for Advanced Studies, DIAS Dunsink Observatory, Dublin D15 XR2R, Ireland
[2]School of Physics, University College Dublin, Belfield, Dublin 4, Ireland
[3]ESA, ESTEC, Noordwijk, Netherlands
[4]Swedish Institute of Space Physics (IRF), Uppsala, Sweden
[5]Max-Planck-Institute for Solar System Research, Göttingen, Germany
[6]Laboratoire de Physique et Chimie de l'Environnement et de l'Espace (LPC2E), CNRS, Orléans, France
[7]Laboratoire Lagrange, Observatoire de la Côte d'Azur, Université Côte d'Azur (OCA), CNRS, Nice, France

Correspondence: Maryam Zeroual (maryam.zeroual@dias.ie)

Abstract.

The JUICE spacecraft performed an Earth gravity assist during the 20-21st August 2024 encountering a range of different plasma environments. An understanding of the surface charging of the spacecraft is important in increasing the scientific output of the instruments, allowing for the development of correction techniques. The surface charging in two of these environments, in the plasmasphere at closest approach (2.07 R_E) and in the magnetosheath, was explored through simulations using the SPIS software. The average surface charging of the conductive surface was found to charge negatively in the plasmasphere to -2 V and positively in the magnetosheath to 2.5 V. Differential charging was observed in both environments due to different materials covering the spacecraft, with the dielectric materials charging from -0.8 to -6 V in the plasmasphere and 7 to -70 V in the magnetosheath. The effect of the spacecraft on the particle environment was also studied, looking at the formation of ion wakes and the photoelectron cloud. In the plasmasphere, the impact of exposed potentials on the solar array was also studied and found not to have any significant effect on the overall charging of the spacecraft. The results obtained here during the Earth swing-by can also be applied when JUICE performs later gravity-assists again at the Earth and the results will be relevant when encountering similar environments at Jupiter and its moons.

1 Introduction

During the 19th to the 20th August 2024, the JUICE spacecraft performed a double gravity assist with both the Moon and the Earth. This marked the first time that the novel manoeuvre referred to as a Lunar Earth Gravity Assist (LEGA) was performed. As well as altering the trajectory of JUICE and making significant fuel savings in its journey to JUICE, the LEGA allowed for the collection of scientific data around both bodies. The Earth encounter is the focus of this study, which aims to support the data analysis of science data collected in the magnetosphere through surface charging analysis.

https://doi.org/10.5194/egusphere-2026-2068
Preprint. Discussion started: 21 April 2026

Interest in surface charging studies is often driven by the risk of hardware damage from electrostatic discharge arising from differential charging of the spacecraft. However, another key region of interest in these studies is due to their impact on the science data collected by the instruments, in particular on the particle and field measurements made. A surface charge can be acquired by the spacecraft from interactions with its environment and may be described by a current balance equation where the sum of the total currents into and out of the spacecraft is 0 at equilibrium; for extensive reviews on surface charging, see (Garrett (1981), Whipple (1981), Minow et al. (2024)). These currents are typically from the absorption of electrons and ions, and the emission of photoelectrons and secondary electrons but other contributors exist for certain environments such as charged dust. In the majority of environments typically encountered by spacecraft the cold electrons will be the dominating contributor to the current balance ~~here~~. This will drive the spacecraft to negative potentials unless the photoelectrons are more dominant ~~here~~. Understanding the overall contribution to the surface charging in different environments and the effect of the spacecraft on local particle populations can be done through the use of the SPIS software (Sarrailh et al. (2015)). Examples of studies using SPIS include Michelagnoli et al. (2024), which looks at the surface charging of the Ariel spacecraft in different L2 relevant environments, Bergman et al. (2020) looking at the effect of different potentials on the Rosetta spacecraft on the ion trajectories and Bergman et al. (2023) simulating the surface charging on the probe B1 of Comet Interceptor. Studies using SPIS have also been applied to JUICE, where Bochet et al. (2023) analyses the effect of surface charging on distortion on the Jovian plasma Dynamics and Composition analyser (JDC) on JUICE, and Holmberg et al. (2024) studying the surface charging on JUICE in the solar wind at 1 AU. Here we study the surface charging and effect on the particle environment of JUICE in the Earth's plasmasphere and magnetosheath for the first time. The results from this will be important in future work in optimising the data output from the JUICE instruments and anticipating the data results that can be obtained. As JUICE continues its mission towards Jupiter, results from these studies can be applied to the environments of Jupiter and its moons where similar compositions exist.

2 The JUICE Mission

2.1 JUICE Earth Swing-by

The JUICE mission is a large class mission selected in 2012 under ESA's Cosmic Vision program, and launched on the 14th April 2023. JUICE marks the first mission to the outer Solar System led by an agency other than NASA. The overall aim of the mission is to improve current understanding of the Jovian system and study the potential habitability of its icy moons. The spacecraft will arrive at Jupiter in 2031 entering a "Jupiter Tour" including 35 flybys of its moons. In 2034 JUICE will enter into orbit around Ganymede for 9 months as its final objective, becoming the first spacecraft to orbit a moon other than Earth's. A detailed overview of the JUICE mission and its objectives is given in Grasset et al. (2013).

As part of its journey to Jupiter, in August 2024 JUICE performed a swing-by of the Moon and then the Earth one day later, referred to as a Lunar Earth Gravity Assist (LEGA) as described in Boutonnet et al. (2024). The spacecraft was the first to complete this novel manoeuvre. Due to the short time span between the Moon and Earth swing-bys, any deviations in the trajectory at the Moon could be further magnified at Earth. This required a concentrated campaign extending over 2

https://doi.org/10.5194/egusphere-2026-2068
Preprint. Discussion started: 21 April 2026

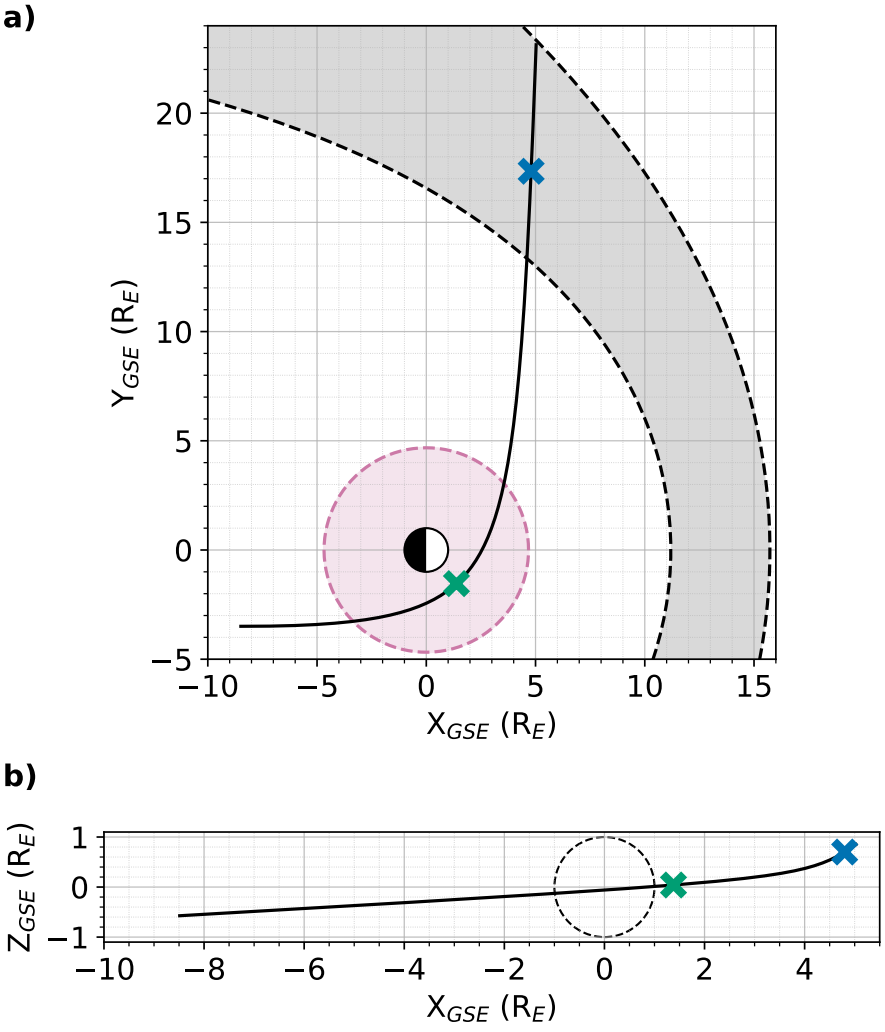

Figure 1. Trajectory of the JUICE spacecraft (solid black line) during the Earth swing-by in Geocentric Solar Ecliptic (GSE) coordinates from the 20th August 2024 19:00 UTC to the 21st August 2024 07:00 UTC with the spacecraft moving out into the solar wind. Panel (a) is the trajectory in the XY plane with the magnetosheath indicated by the shaded grey region between the dashed black lines marking the magnetopause and bow shock. These were illustrated using a simple model by Chao et al. (2002). The plasmasphere region has been indicated by the shaded pink region with the dashed line indicating the plasmapause, using Carpenter and Anderson (1992) and Kp = 2. Panel (b) shows the trajectory in the XZ plane, during the same period. The blue and green crosses in both panels show the locations chosen to analyse the surface charging in. Blue is the location X_{GSE} = 4.80, Y_{GSE} = 17.34, Z_{GSE} = 0.70 where the spacecraft was located at 04:30 in the magnetosheath. Green marks the closest approach at 21:56 with coordinates X_{GSE} = 1.38, Y_{GSE} = -1.54, Z_{GSE} = 0.041.

months however the resulting swing-by was conducted successfully. The LEGA manoeuvre allowed for significant savings of propulsive fuel, which can be used later in the mission to extend scientific output. As well as saving fuel, the LEGA also

https://doi.org/10.5194/egusphere-2026-2068
Preprint. Discussion started: 21 April 2026

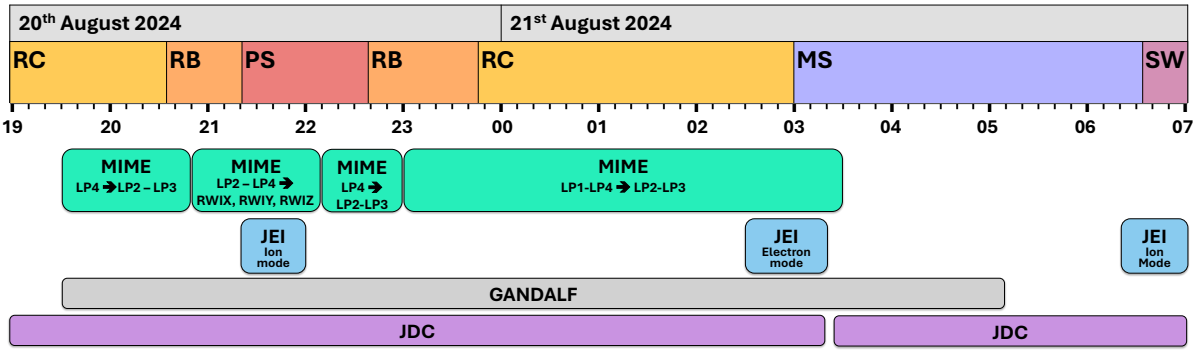

Figure 2. Timeline highlighting the different plasma environments encountered by JUICE during the Earth swing-by from the 20th August 2024 19:00 UTC to 21st August 2024 07:00 UTC and the different particle and field instruments that were switched on at the time. The times marking the ring current (RC), radiation belt (RB), plasmasphere (PS), magnetosheath (MS) and solar wind (SW) boundaries are approximate and based on available spacecraft data. The Mutual Impedance MEasurement Experiment (MIME) shown in green, is a part of the RPWI Instrumentation, using the 4 Langmuir probes (LP1-LP4) and the three dipole antennas (RWI), as described in Wahlund et al. (2024). GANDALF (grey) describes another RPWI experiment using the LP probes and LP receiver. The JEI sensor (blue) and the JDC sensor (purple) are a part of the PEP instrument package.

allowed for the collection of scientific data, with all instruments switched on during the Moon swing-by and 8 out of 10 instruments switched on during the Earth swing-by.

The trajectory of the spacecraft during the Earth swing-by is illustrated in Figure 1, from the 20th August 2024 19:00 to the 21st August 2024 07:00 UTC, after which the spacecraft entered the solar wind. The coordinates shown are in Geocentric Solar Ecliptic (GSE) coordinates, which are defined as:

- X_{GSE} is pointing towards the Earth-Sun line
- Y_{GSE} completes the right hand system
- Z_{GSE} perpendicular to ecliptic plane of date in the northward direction

The trajectory of the JUICE spacecraft during the Earth swing-by allowed it to explore various plasma environments around the Earth including the plasmasphere and magnetosheath indicated by the pink and the grey shaded regions in Figure 1a. The various space environments encountered during the Earth swing-by is also illustrated by the timeline of the spacecraft and its particle and field observations shown in Figure 2. The effects of the surface charging in these different environments will be varied due to their different plasma properties, including changing temperatures and densities, and this difference can be quantified through the simulations performed. These predicted results can also be compared against any available instrument data. Two regions of interest were selected to perform SPIS simulations, one in the plasmasphere during closest approach at time 21:56 and position X_{GSE} = 1.38, Y_{GSE} = -1.54, Z_{GSE} = 0.041 (19° magnetic latitude (MLat) and 08:40 magnetic local

https://doi.org/10.5194/egusphere-2026-2068
Preprint. Discussion started: 21 April 2026

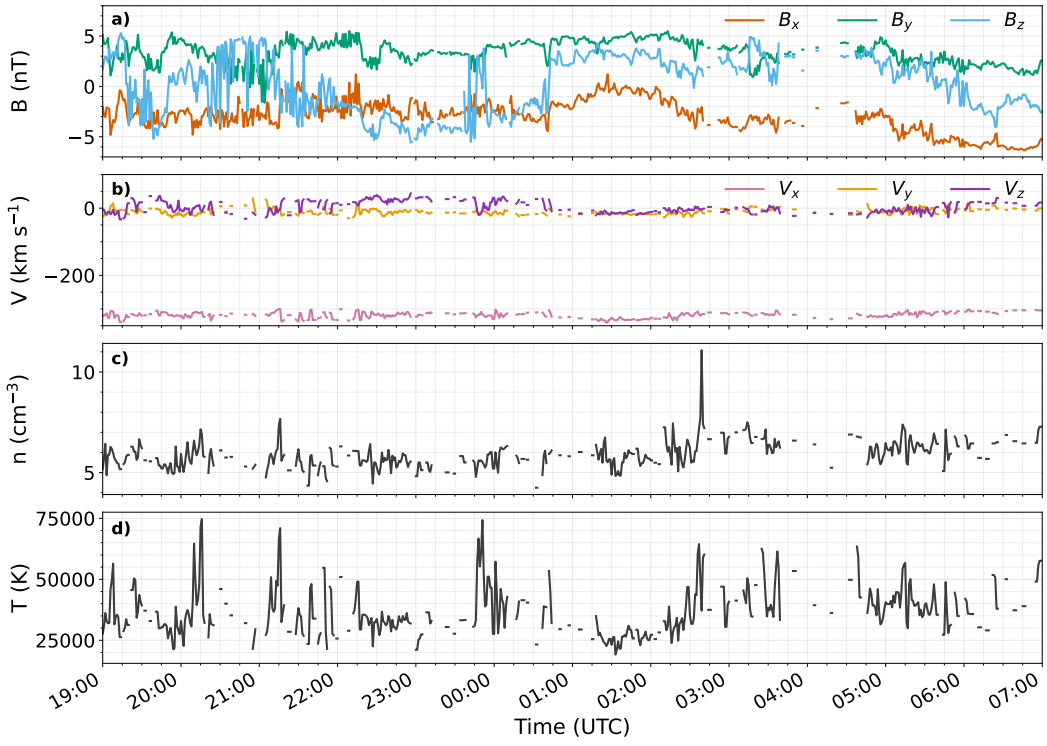

Figure 3. Solar wind parameters from the OMNI dataset at 1-min resolution from the 20th August 2024 19:00 UTC to 21st August 2024 07:00 UTC during the Earth swing-by. (a) The magnetic field components B_x, B_y and B_z. (b) The velocity components V_x, V_y and V_z. (c) The number density and (d) the solar wind temperature.

time (MLT)) indicated in Figure 1 by the green cross. The second chosen location is in the magnetosheath at 04:30 and X_{GSE} = 4.80, Y_{GSE} = 17.34, Z_{GSE} = 0.70 and is marked by the blue cross. Input parameters for the SPIS simulations must be obtained for each region, with the main challenge arising in characterising the environment through the global parameters. The solar wind conditions provide some information as to the environment experienced by JUICE particularly in the magnetosheath, and the subsequent surface charging that will be obtained. Figure 3 illustrates the solar wind parameters obtained during the Earth swing-by, using data obtained from the OMNI dataset and accessed via OMNIWeb. The parameters observed represent relatively undisturbed, slow solar wind conditions without any significant variability seen. Additionally, instrument data from JUICE itself can be used to characterise the environment, however at this early stage the data is not yet fully calibrated so should be used with care before the final data products are available. Environment parameters from statistical data or other various models may provide a more robust estimation of the average plasma environment. A combination of all models and instrument data is used to provide the best possible description of the plasma environments to be used as inputs to the SPIS simulations.

https://doi.org/10.5194/egusphere-2026-2068
Preprint. Discussion started: 21 April 2026

2.2 Spacecraft Model and Instruments

To perform science measurements within the Jupiter system, JUICE has a total of 10 instrument packages, as illustrated in Figure 4. There is also an additional experiment being carried out using existing hardware named the Planetary Radio Interferometer and Doppler Experiment (PRIDE). Of these instrument packages, those carrying out particle and field measurements will be most affected by surface charging. These instruments are the Radio and Plasma Wave Investigation (RPWI), the JUICE Magnetometer (J-MAG), and the Particle Environment Package (PEP). In the near-Earth environment the impact on J-MAG will be negligible. This is as the currents to and from the spacecraft will produce magnetic fields much smaller than the ambient magnetic field in the different environments explored here. PEP consists of 6 sensors to measure neutral and charged particles. This includes the Jovian plasma Dynamics and Composition (JDC) analyser, the Jovian Electrons and Ions (JEI) analyser and the Neutral gas and Ion Mass (NIM) spectrometer, which all measure the properties of cold plasma. The Radio and Plasma Wave Investigation (RPWI) is designed to focus on the cold plasma populations (< 100 eV) and electromagnetic fields. RPWI consists of 10 individual sensors which are divided into 3 groups depending on the measurements they perform. One of these groups includes the 4 Langmuir probes (LP1-LP4).

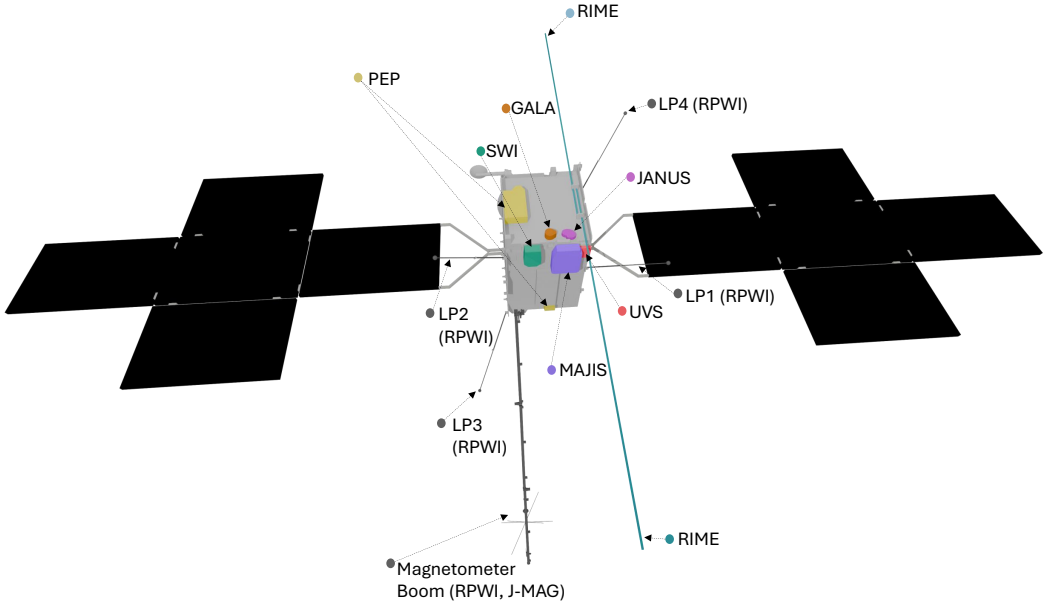

Figure 4. Illustration of the JUICE spacecraft indicating the locations of the different instrumentations on the spacecraft. 3GM is contained inside the spacecraft so is not shown here.

The remaining instruments can be divided into two broad categories. the first is the optical instruments consisting of the camera JANUS, the Moons and Jupiter Imaging Spectrometer (MAJIS), the UV spectrometer (UVS) and the Sub-millimetre Wave Instrument (SWI). The remaining are the geophysical instruments, the Ganymede Laser Altimeter (GALA), the Radar

https://doi.org/10.5194/egusphere-2026-2068
Preprint. Discussion started: 21 April 2026

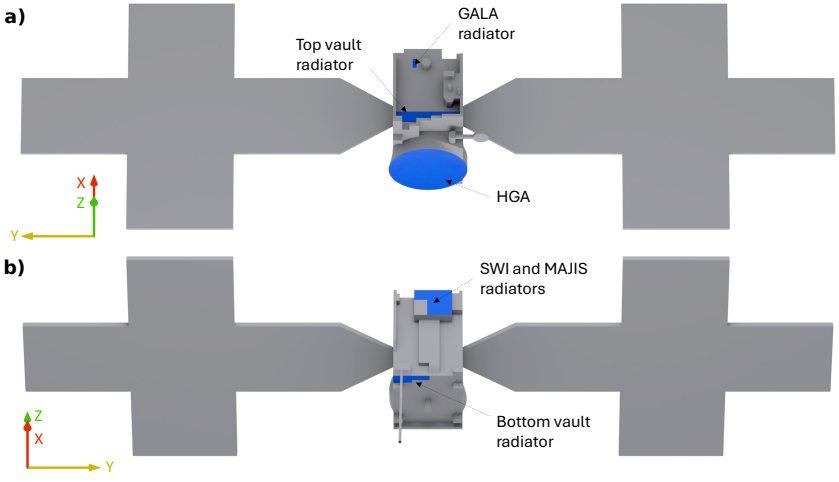

Figure 5. Figure showing the simplified spacecraft model used in the SPIS simulations. The grey indicates the conductive material of the spacecraft and blue the dielectric materials which will charge to different potentials to the conductive surfaces. a) Shows the front and top view of the spacecraft including the HGA, top vault radiator and GALA radiator as indicated by the arrows. b) Rear view of the spacecraft including the bottom vault radiator and the SWI and MAJIS radiators.

for Icy Moons Exploration (RIME) and the Gravity and Geophysics of Jupiter and the Galilean Moons (3GM) radio science package. These instruments are not expected to be significantly affected by surface charging effects, and so are not considered any further here.

In order to perform the simulations using SPIS, a model of the JUICE spacecraft is required. This is described in detail in Holmberg et al. (2024), here the key components will be briefly detailed. Figure 5 shows the front and rear view of the model used for the simulations. A coordinate system has been defined where

- X lies opposite the High-Gain Antenna (HGA) direction
- Y along the solar panels
- Z completing the right hand side system

Following the official JUICE spacecraft coordinate system, the origin is at 1.73 m below the centre of the HGA just below the spacecraft in Z.

Defined in the model is the spacecraft bus at 2.25 × 2.50 × 3.52 m, the HGA of diameter 2.54 m, and the solar panels which span a length of 12.07 m in Y and 7.44 m in Z. The solar panels are tilted at an angle of 70°, as this was their orientation in both the plasmasphere and magnetosheath. Some simplifications to the model have been made as required to reduce the simulation time whilst maintaining the accuracy of the results. One example of this is the exclusion of the Langmuir probes, which would have no significant impact on the surface charging due to their small area and conductive surface. The relevant materials for

https://doi.org/10.5194/egusphere-2026-2068
Preprint. Discussion started: 21 April 2026

our study used in the spacecraft model are also illustrated in Figure 5 with blue highlighting the dielectric surfaces and grey the conductive. The dielectric material here is the white paint Z93C55 which covers the radiators and HGA. A more detailed description of all the materials used is given in Holmberg et al. (2024).

3 Characterising the Environment

3.1 Magnetosheath Environment

During the Earth swing-by, JUICE encountered various regions of Earth's plasma environment taking measurements with the available instruments on board, as indicated previously in Figure 2. One of the plasma environments of interest is within the magnetosheath, which has been selected for the SPIS simulations. This marks the region where the previously supersonic solar wind has been slowed to subsonic speeds by the bow shock. Continuing inwards towards the Earth, we encounter the magnetopause, which defines the innermost boundary of the magnetosheath. The JUICE spacecraft first entered the magnetosheath on the 21st August 2024 at approximately 03:00. The spacecraft then remained in the magnetosheath for over 3 hours until it crossed the bow shock into the solar wind. The properties of the magnetosheath are highly variable, and determined both by the incoming solar wind conditions and the location within the magnetosheath. Typically, incoming solar wind follows a Parker spiral configuration. This geometry results in asymmetries in the properties of the magnetosheath referred to as dawn dusk asymmetries. Therefore, to accurately characterize the environment within the magnetosheath, it is important to consider the location within it. We selected one region of focus at 04:30 at X_{GSE} = 4.80, Y_{GSE} = 17.34, Z_{GSE} = 0.70 as described in subsection 2.1.

To perform the simulations, an accurate representation of the environment is required. This was done primarily using a statistical model of the magnetosheath developed by Ma et al. (2020), known as the Solar Wind and Magnetosphere Unification (SAMU) model. SAMU is an empirical model, utilising data from the THEMIS mission between August 2007 and March 2020. To negate the effects of boundary motion in the magnetosheath, they utilised a normalised coordinate system allowing for direct comparison of THEMIS data collected under different solar wind conditions. The normalisation process made use of the 3-D bow shock model by Verigin et al. (2001) and the magnetopause model by Shue et al. (1998). Results from the SAMU model were then compared by Ma et al. (2020) against the MHD model BATSRUS. Both models showed similar large scale patterns however, the SAMU model was able to capture smaller scale effects not reproducible through MHD modelling. Using the SAMU model, the parameters used for the simulations were obtained and are contained within Table 1. To select the relevant data from the SAMU model for the magnetosheath region, the location of the data used was restricted to $\pm$ 0.5 radii around the spacecraft in normalised coordinates. An additional criteria was applied limiting the points chosen based on the solar wind conditions. This solar wind range was chosen to mimic that at the JUICE spacecraft at the time of interest as illustrated in Figure 3, whilst maintaining a wide enough range to obtain enough data for each required magnetosheath parameter.

To ensure the accuracy of the parameters that will be used to represent the magnetosheath environment, additional parameters were also obtained using the MHD models BATSRUS and OpenGGCM as indicated in Table 1. In general, the different parameters obtained by the various models lie within a close range to each other, with any variabilities having a limited impact

https://doi.org/10.5194/egusphere-2026-2068
Preprint. Discussion started: 21 April 2026

Parameter	Units	Input value	SAMU	BATSRUS	OpenGGCM
n	cm^{-3}	19.4	19.4	18.7	16.2
T_e	eV	17.7	17.7	-	-
T_i	eV	94.1	94.1	108.6	114.4
$v_{p,x}$	km/s	-155	-155	-187	-191
$v_{p,y}$	km/s	119	119	68	78
$v_{p,z}$	km/s	-33	-33	-66	-3
B_x	nT	-9.1	-	-9.1	-8.8
B_y	nT	16.8	-	16.8	12.1
B_z	nT	1.7	-	1.7	5.5

Component	Units	Value	References
$v_{s/c,x}$	km/s	0.18	
$v_{s/c,y}$	km/s	4.21	Spacecraft velocity values obtained from operational data
$v_{s/c,z}$	km/s	0.11	

Table 1. Table containing parameters used for the SPIS simulations of the JUICE spacecraft in the magnetosheath on the 21st August 2024 04:30 UTC. The number density is the same for electrons and ions using the assumption of a quasi-neutral plasma environment. All values here are given in GSE coordinates.

on the surface charging that would be obtained by JUICE. As there is no available SAMU data for the magnetic field parameters at this location, values from the BATSRUS model were input here instead.

3.2 Plasmasphere Environment

The second plasma environment considered for SPIS simulations is within the plasmasphere as described in subsection 2.1. The plasmasphere describes the inner region of the magnetosphere containing cold dense plasma that forms a torus-like structure around the Earth, illustrated with the pink region of Figure 1. The plasma within is largely of ionospheric origin, composed primarily of hydrogen (∼80%) ions (Lemaire and Gringauz (1998)) as well as helium and oxygen ions. Close to Earth, the magnetic field structure is approximately dipolar and the motion of the plasma is dominated by the co-rotation electric field. The magnetospheric convection field, which arises from solar wind and magnetosphere interactions is influential in the formation of the plasmapause. The plasmapause defines the plasmasphere's outer boundary, and its location varies strongly with geomagnetic activity, expanding in size during quiet times.

During the Earth swing-by, JUICE first entered the plasmasphere on the 20th August 2024 around 21:15, where it remained in this region for approximately 1 hour 30 minutes with the trajectory illustrated in Figure 1. The closest approach of the

https://doi.org/10.5194/egusphere-2026-2068
Preprint. Discussion started: 21 April 2026

Parameter	Units	Input value	Reference values	References
$n_{e,c}$	cm^{-3}	2400	1900, 1500, 2100, 1800, 1670, 2400	Ripoll et al. (2024), Carpenter and Anderson (1992), Ozhogin et al. (2014), Singh et al. (1998), RPWI/MIME, RPWI/LP
$T_{e,c}$	eV	0.50	(0.42 - 0.64), 0.54, 0.69, 0.50	Balan et al. (1996), Abe et al. (1997), Kutiev et al. (2002), RPWI/LP
$n_{e,w}$	cm^{-3}	160	160	RPWI/LP
$T_{e,w}$	eV	2.8	2.8	RPWI/LP
n_i	cm^{-3}	2560	(1500 - 4500)	Goldstein et al. (2019)
T_i	eV	0.45	0.53, (0.36 - 0.65), 0.45 (0.28 - 0.55), (0.18 – 0.28)	Craven et al. (1991), Goldstein et al. (2019), Comfort (1996), JEI
$v_{p,x}$	km/s	1.23		
$v_{p,y}$	km/s	1.11	10 %, 10-15 % co-rotation	Zhang et al. (2024), Sandel et al. (2003)
$v_{p,z}$	km/s	0.13		

Component	Units	Value	References
$v_{s/c,x}$	km/s	6.24	
$v_{s/c,y}$	km/s	5.65	Spacecraft velocity values obtained from operational data
$v_{s/c,z}$	km/s	0.50	
B_x	nT	-1530	
B_y	nT	1760	International Geomagnetic Reference Field (IGRF) model of magnetic field
B_z	nT	3440	

Table 2. Parameters used for the SPIS simulations in the plasmasphere at closest approach. The values in brackets indicate the range where available. Vectors given are in GSE coordinates

spacecraft to Earth occurred within the plasmasphere at 21:56 at a distance of 2.07 R_E corresponding to an altitude of 6833 km above the Earth's surface. Here JUICE was located at X_{GSE} = 1.38, Y_{GSE} = -1.54, Z_{GSE} = 0.041 in GSE coordinates (MLat = 19° MLT = 08:40), as stated in subsection 2.1. The time of closest approach is of interest, as it is the region that would typically contain the densest plasma and is a location where several key instruments were switched on. For these reasons, this time was chosen to conduct the surface charging simulations in. To describe the plasma environment here for the SPIS simulations, parameters from a variety of studies were utilised, presented in Table 2.

To represent the plasmasphere environment, parameters have been obtained from a variety of ground based instrument and spacecraft data and models from these. As the plasmasphere environment varies depending on magnetic field conditions, a field line tracing method was used to determine the typical environment at this time using the SuperMAG online interface[

https://doi.org/10.5194/egusphere-2026-2068
Preprint. Discussion started: 21 April 2026

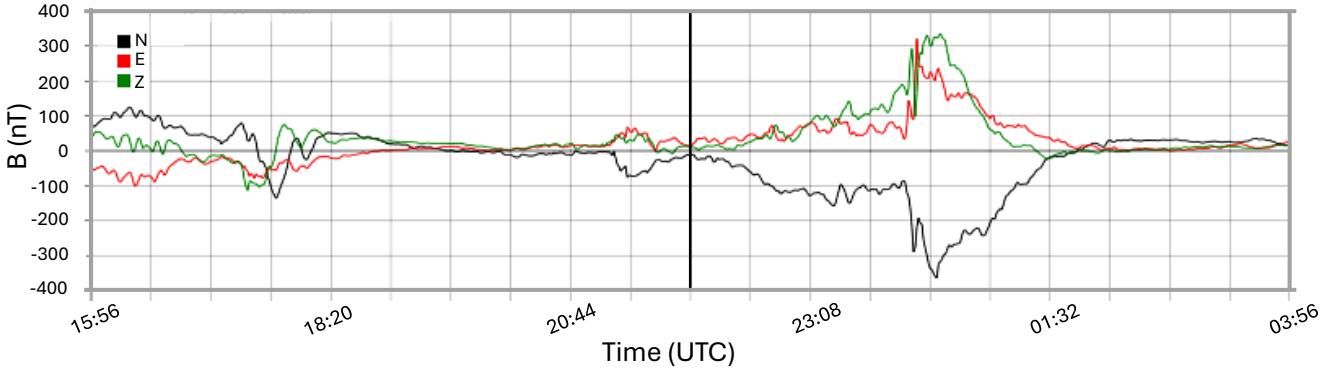

Figure 6. Magnetic field data from the Kevo magnetometer in the northern hemisphere from the 20th August 15:56 to the 21st August 03:56. The different components in the local magnetic north, N, and east, E, are indicated in black and red respectively whilst the green is vertically downwards, Z. The black vertical line in the figure indicates the closest approach time for JUICE.

https://supermag.jhuapl.edu/line/]. This followed the field lines from JUICE using the tsyganeko89 and IGRF model in the northern and southern hemispheres, as implemented in the Python module geopack (Tian et al. (2025)). Through this method 5 magnetometers were found available around +/- 10 geographic latitude and longitude of root of the field lines in the northern hemisphere ionosphere; 3 magnetometers were found within +/- 30 in the southern hemisphere ionosphere. From the southern hemisphere magnetometers observe a very calm period with almost no activity seen here. The northern hemisphere magnetometers show a potential substorm starting at around 23:00, see Figure 6. However, this will not affect JUICE which is located in the dayside sector. This event may also be due to dayside driving which will have a limited impact on the spacecraft itself. Based on the presented magnetometer data, we can therefore conclude that the environment is characterised by a period of quiet geomagnetic activity, which will be reflected in the parameters obtained to describe the environment.

The cold electron density values have been obtained from studies using data from the EFW instrument on the Van-Allen probes, IMAGE RPI measurements, ISEE data and ground based whistler observations from Tihany. Additionally, the RPWI/MIME and RPWI/LP experiments on JUICE returned electron density values which are in good agreement with the previous studies. A warm population of electrons was also observed by the RPWI instrument with a high density, which will also be included in the simulations. The ion density value was chosen assuming a quasi-neutral environment. Ion densities were also observed by the Dynamics Explorer-1 (DE-1) Retarding Ion Mass Spectrometer (RIMS) which gives results in good agreement with the assumption of quasi-neutrality in this region. Ion temperature was also obtained from work using the DE-1

https://doi.org/10.5194/egusphere-2026-2068
Preprint. Discussion started: 21 April 2026

RIMS mission and from data on the JEI instrument on JUICE. The cold electron temperature was found from studies using data from the Akebono spacecraft. Due to the cold temperature of the plasmasphere at this distance, studies finding plasmasphere parameters such as the electron temperature ~~can be~~ limited. This is due to the difficulties associated with measuring this data including photoelectron contamination which can obscure the background electron population as described in Maldonado et al. (2023). To find the magnetic field components the International Geomagnetic Reference Field (IGRF) model was used, which mathematically characterises the field around Earth. Plasma velocities were calculated assuming co-rotation with the Earth with a lag as described by the studies obtained.

A hot population also exists in the plasmasphere as described in Rasinskaite et al. (2025) with energies on the order of 100 keV and low densities. Due to these low densities this population was not found to significantly impact the surface charging of the spacecraft so is not included in the final environment description used for the simulations.

4 Results and Discussion

4.0.1 Results in the Magnetosheath

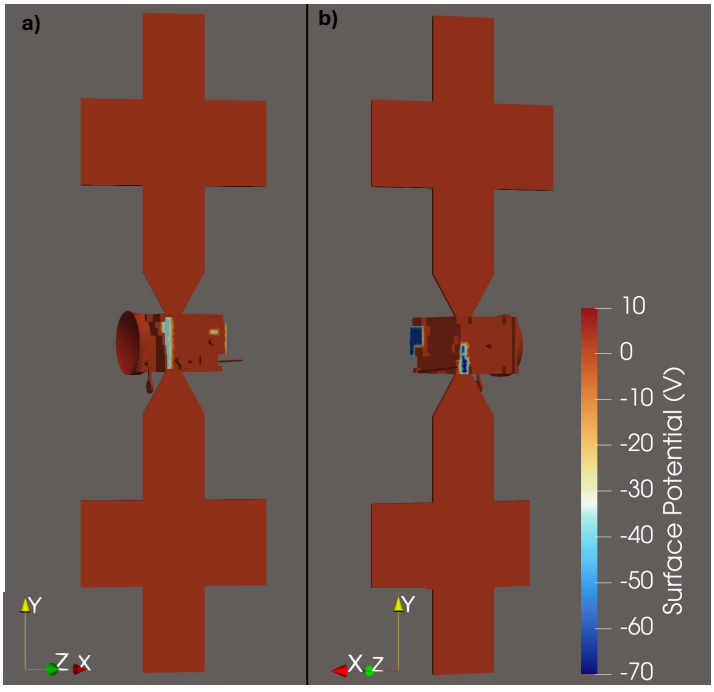

Figure 7. The simulated surface potential of JUICE in the magnetosheath during the 21st August 2024 at 04:30. The conductive surface reaches a potential of 2.5 V. The highest positive potential is achieved by the HGA which reaches a potential of 7 V. The greatest negative charge is obtained by the bottom vault radiator at -70 V.

https://doi.org/10.5194/egusphere-2026-2068
Preprint. Discussion started: 21 April 2026

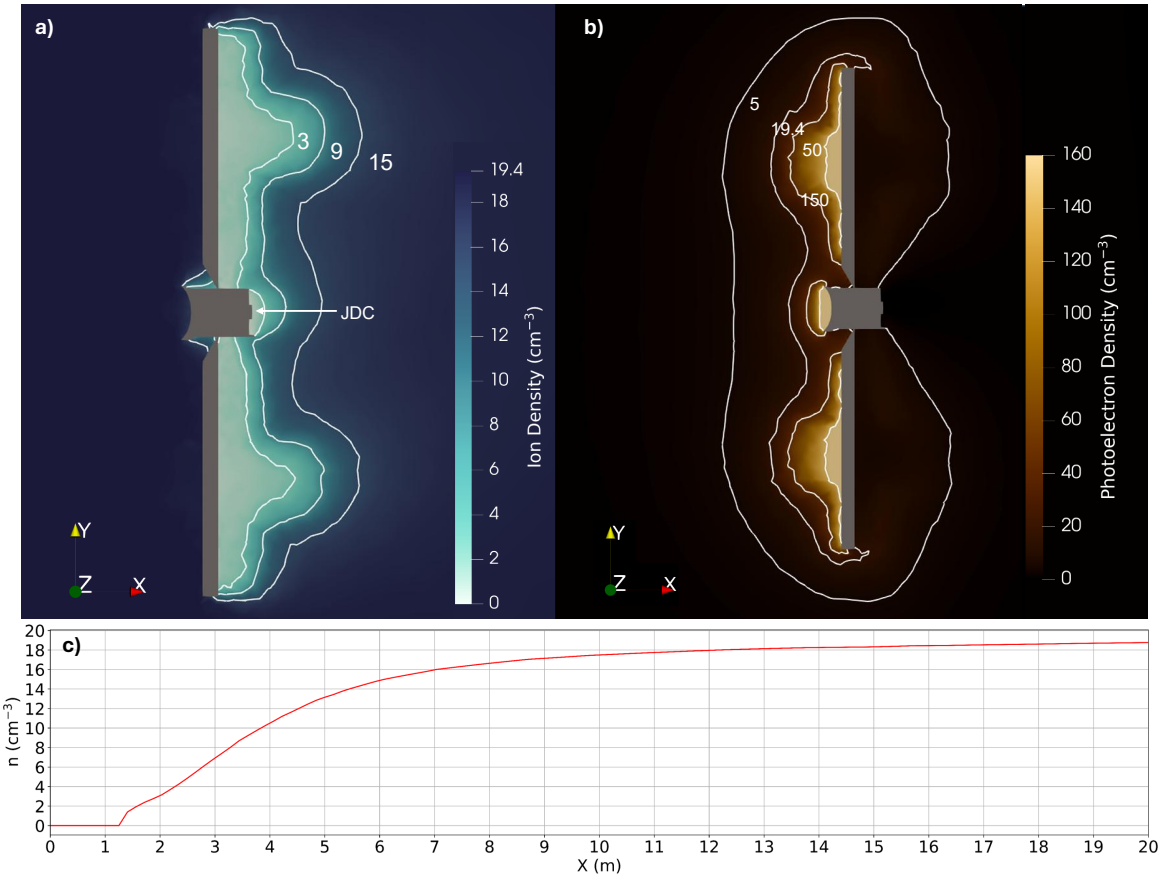

Figure 8. a)Cross section of JUICE illustrating the formation of a minor ion wake. The white contour lines indicate the densities at 3, 9 and 15 cm^{-3} moving out from the spacecraft. The arrow indicates the JDC instrument located within the wake. b) Simulated photoelectron densities around JUICE whilst in the magnetosheath. The white contour lines indicate densities of 5, 19.4, 50 and 150 cm^{-3}. c) Ion density following a line outward from the spacecraft, crossing the JDC instrument and outwards along the X axis. The initially reduced ion densities in comparison to the background value of 19.1 cm^{-3} indicate the presence of an ion wake extending for $\sim$ 10 m.

https://doi.org/10.5194/egusphere-2026-2068
Preprint. Discussion started: 21 April 2026

Surface charging results on JUICE were obtained in the magnetosheath environment through the SPIS simulations conducted, as presented in Figure 7. The simulations in this environment used a full kinetic treatment of the particle populations through the Particle-In-Cell (PIC) method. The conductive surface of the spacecraft, that is the spacecraft bus and solar panels, obtained an overall positive charge of 2.5 V as shown in Figure 7, panel a and b. In this environment the emission of photoelectrons dominates the resulting potential leading to the positive potential seen. The dielectric surfaces different potentials to the conductive surfaces. The greatest positive potential was obtained by the HGA, charging to ∼7 V, see Figure 7a. The antenna is directed towards the Sun, so the emission of photoelectrons has a large impact on the instrument. The greatest negative charge was found by the bottom vault radiator located on the -Z side of the spacecraft. This reached a potential of ∼-70 V, see Figure 7b. This radiator was shielded from the Sun so emitted no significant amount of photoelectrons, but still accumulated a negative charge through its interaction with electrons in the plasma. The position and material of the surfaces on the JUICE spacecraft impact significantly the resulting potential obtained. However, the orientation with the HGA pointing towards the Sun is the one that is maintained within 1.3 AU, as this is a requirement for thermal control of the spacecraft. The contribution of secondary electrons has not been included in these simulations, as they currently are not correctly represented in SPIS for cold plasma and may lead to incorrect results being obtained. However, their presence may have some limited impact on the potentials obtained in the magnetosheath, particularly for the radiators. A simulation including the SPIS modelled secondary electrons, which currently overestimates secondary electron production, obtains a difference in the potential of ∼1.4 V for the conductive surface, ∼0.5 V for the HGA and ∼40 V for the bottom vault radiator, not shown. The secondary electrons will therefore have a limited impact on the HGA and conductive surfaces driving them to more positive potentials. The most significant impact will be on the radiators of the spacecraft which will become less negative through the secondary electron production. The values given for the differences are overestimates of the impact, due to the current modelling of secondary electron production in SPIS, so whilst they are expected to have some impact, it will likely not be as significant as currently described here.

The results for the surface charging here have been presented for a particular time at 04:30 while JUICE was in the magnetosheath in the position illustrated in Figure 1. However, to test the sensitivity of the spacecraft different periods were also simulated including at 03:30 with X_{GSE} = 4.69, Y_{GSE} = 14.95, Z_{GSE} = 0.63 and 05:00 at X_{GSE} = 4.85, Y_{GSE} = 18.52 and Z_{GSE} = 0.73. These different time periods had a limited impact on the overall charging of the spacecraft, with the maximum change in the conductive surface of the spacecraft reaching 1 V. The time chosen at 04:30 is therefore a good representation of the overall behaviour the spacecraft will observe whilst in the magnetosheath.

As well as obtaining potentials for JUICE the SPIS simulations can output several other pieces of information to understand the behaviour of the spacecraft. One of these is the behaviour of the ion density around the spacecraft illustrated in Figure 8a. Here an ion wake can be observed which is formed since the relative speed between the spacecraft and ions is larger than the thermal energy of the ions. A wake may also be formed due to the potential of the spacecraft (Engwall et al. (2006)), but in this case the potential is small and the dominant cause of the ion wake formation is from the spacecraft acting as an obstacle to the plasma flow. The wake itself is relatively small in dimension spanning approximately 10 m from the rear of the spacecraft as shown in Figure 8c which traces the ion density following a line starting from the centre of the spacecraft, crossing the location

https://doi.org/10.5194/egusphere-2026-2068
Preprint. Discussion started: 21 April 2026

of the JDC instrument and extending in the spacecraft X direction beyond this. The JDC instrument is located within this wake, so will see a reduced density reading than otherwise expected.

The density of emitted photoelectrons is also obtained through the SPIS simulations. Figure 8b illustrates the formation of the photoelectron cloud around the spacecraft. A maximum density is obtained above the HGA of over 400 cm^{-3}. The photoelectrons are also attracted back to the spacecraft due to its positive charge, so they extend to the rear of the spacecraft as well. The presence of these photoelectrons can impact the electron measurements made, particularly of low energy electrons obscuring the measurements made here. An example of this is in the measurements made by the JEI instrument on-board JUICE, where a constant photoelectron background can be observed.

4.1 Results in the Plasmasphere

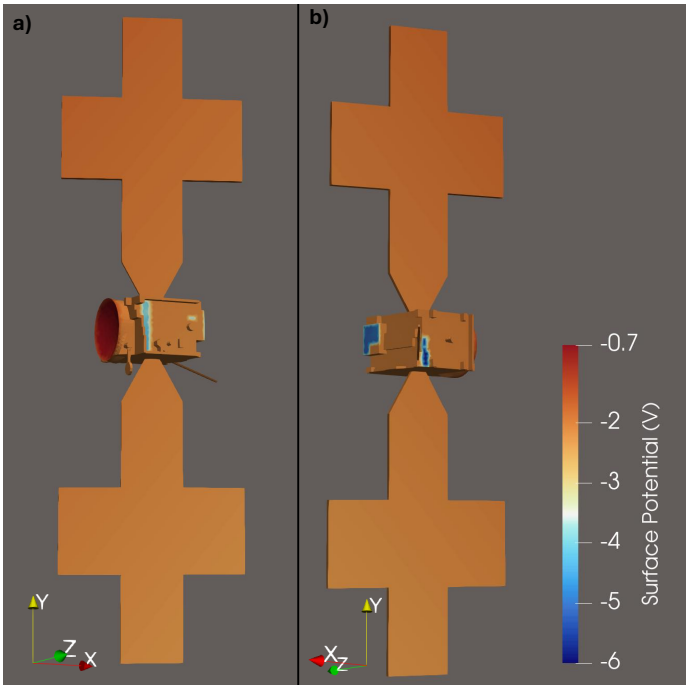

Figure 9. The surface potential of JUICE at closest approach in the plasmasphere during the 20th August 2024 at 21:56 UTC. The conductive surface reaches a potential of -2 V. The greatest potential is achieved by the HGA at -0.8 V. The smallest potential is obtained by the bottom vault radiator at -6 V.

Results for the surface potential were obtained for the JUICE spacecraft at the closest approach in the plasmasphere. A hybrid simulation was run for this region, where the cold electron population is modelled using a Maxwell-Boltzmann distribution, as the small Debye length of 0.1 m makes a full PIC simulation very computationally expensive. As in the magnetosheath, secondary electrons have not been included in the simulations. They are also expected to have a very limited impact in a cold and dense environment such as the plasmasphere, so will have a negligible impact on the results obtained. The results for the

https://doi.org/10.5194/egusphere-2026-2068
Preprint. Discussion started: 21 April 2026

surface charging of JUICE in this region are illustrated in Figure 9. Here, the conductive surface of the spacecraft achieves an average overall negative charge of -2 V. An overall negative charge is obtained as the spacecraft resides in a cold dense environment where the current from the collected electrons dominates over the collected ions and emitted photoelectrons. The dielectric materials on the spacecraft charge to different potentials, as in the magnetosheath environment. The maximum surface potential was achieved by the HGA at a potential of -0.8 V, see Figure 9a. This again points towards the Sun, so the full surface will emit photoelectrons resulting in the weaker negative potential. The minimum surface potential was achieved by the bottom vault radiator at around -6 V, see Figure 9b. Even though this radiator is located on the +X side of the spacecraft resulting in no photoemission, the electrons within the dense environment still impact the radiator. This results in a smaller negative potential than seen in the magnetosheath environment.

A slight difference in the lower and upper potentials achieved by the solar panels is also seen, shown in Figure 9 where the potential varies by 0.26 V across both the top and bottom solar panels. The slight decrease in potential is in the -Y and X direction here showing a faint diagonal pattern. This pattern is due to the motional electric field which influences the movement of the cold electrons leading to the slight potential gradient seen. The influence of the motional electric field is also seen in Figure 9b as the photoelectrons move downwards in Y. They also show a slight motion in X but this is suppressed due to the charge on the solar panels. Without the influence of the magnetic field the photoelectron cloud would show a shape similar to that previously illustrated in the magnetosheath, emitted on the front of the spacecraft. The strong influence of the magnetic field in this region means that the photoelectron trajectories will be altered, trailing downwards in the case. This also affects the overall potential that is seen on the lower solar panel, increasing the negative potential here.

The effect of JUICE on the local ion population is illustrated in Figure 10a, showing the ion densities around the spacecraft in the X-Z plane. Here, the formation of a small ion wake can be observed behind the spacecraft due to its motion which is primarily in the -X direction. Additionally, a depletion of ions can also be observed in front of and around the spacecraft as well. The negative charge of the spacecraft results in ions being accelerated towards the spacecraft. The ions in this environment also approach the spacecraft from all directions due to the thermal velocity of the ions which exceeds their co-rotation velocity. Here, geometric blocking of these ions and their absorption will contribute to the overall ion depletion seen around the spacecraft.

The values obtained for the surface charging of JUICE can also be compared with those obtained from the spacecraft itself, including from RPWI and JEI instruments. These were switched on during closest approach as shown previously in Figure 2. The RPWI instrument found potentials between -4.5 to -4.8 V. The JEI data does not yet provide any exact spacecraft potentials, but appears to be more consistent with a slightly less negative potential than reported by the RPWI instrument at around -3.5 to -4 V (Fränz et al. (2026)). The values reported are therefore consistent with the SPIS simulations in showing a small negative charge of the spacecraft, however are of a slightly greater magnitude than reported by the simulations. Whilst it is not expected for the simulations and data to report exactly the same values, as simplifications introduced in the simulations may lead to some discrepancies other factors such as the environment definition or factors in the spacecraft design may also lead to these differences reported. Therefore, an investigation was carried out on this, looking at the effect of exposed conductors on the solar arrays and their influence on the overall surface charging of the spacecraft.

https://doi.org/10.5194/egusphere-2026-2068
Preprint. Discussion started: 21 April 2026

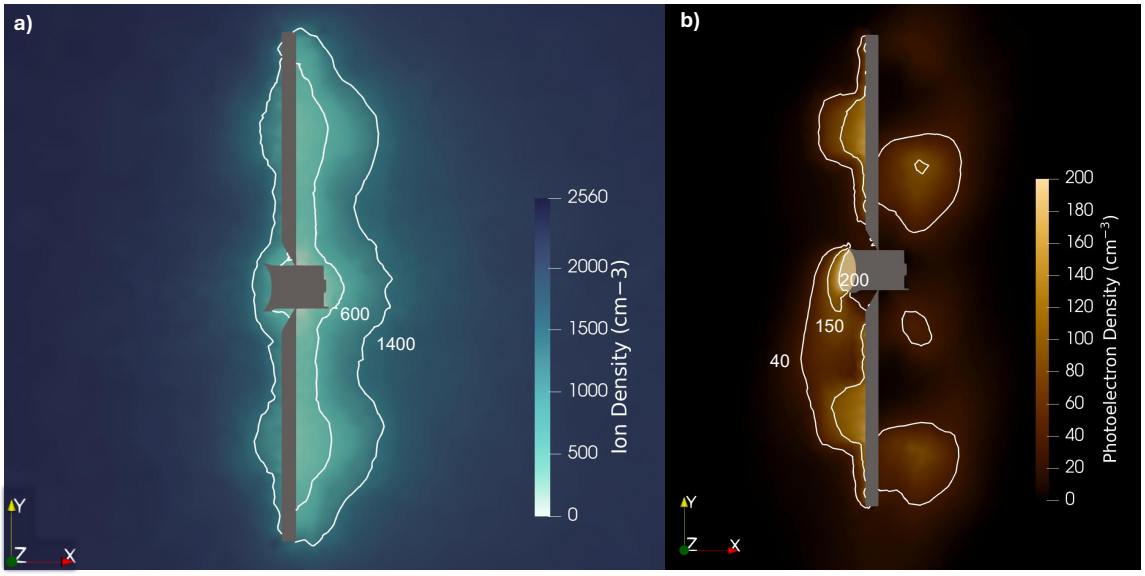

Figure 10. a) Cross section of the JUICE spacecraft illustrating the ion densities around the spacecraft. The white contour lines indicate the densities at 600 and 1400 cm^{-3}. b) Simulated photoelectron densities around the JUICE spacecraft at closest approach. The white contour lines indicate densities of 40, 150 and 200 cm^{-3}

4.1.1 Positively Biased Potentials on the Solar Array

The effect of positively biased exposed potentials (interconnects) on the Rosetta spacecraft has previously been studied in Johansson, F. L. et al. (2020), showing that these can have a significant impact on the overall surface charging of the spacecraft, particularly in cold dense environments. The plasmasphere can be considered to be a cold and dense environment, so the impact of these exposed potentials on JUICE and their overall contribution to the surface charging was considered. Figure 11 shows a simple illustration of the front of a solar panel on the JUICE spacecraft. Here, a panel consists of a total of 126 strings with 42 on each row. One string contains 19 cells with a thin indium tin oxide layer over them. The busbars used to connect the strings gain a maximum potential of 75 V. These strings alternate in direction so that the direction of the potential gradient from 0 to 75 V alternates between each string in a row. JUICE consists of a total of 10 panels and each with the same configuration. Not included in the diagram are the slight variations that result from the positioning of the different holding points in the solar panel.

Using the configuration described, the interconnects were set up in the SPIS software through the groups editor. Excluding the interconnect setup, the same set-up as previously described for the plasmasphere was used in this simulation to illustrate only the effect of the addition of the interconnects. The results are illustrated in Figure 12 showing the potential obtained

https://doi.org/10.5194/egusphere-2026-2068
Preprint. Discussion started: 21 April 2026

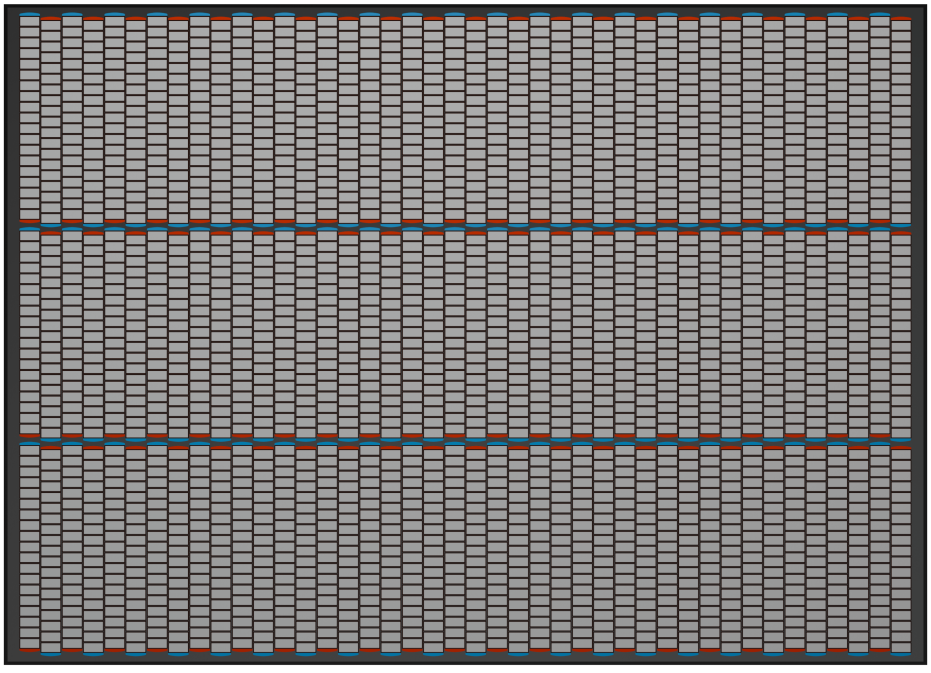

Figure 11. Simplified diagram illustrating the front of the solar panel on JUICE. The blue and red indicate the busbars, with the blue at 0 V and red gaining a potential up to 75 V. The solar panel consists of 3 strings arranged in a column each with 19 cells. Each row of the panel contains 42 strings within it arranged so that the direction of the potential gradient alternates with each string.

with the addition of the interconnects in Panel a and without in Panel b. The range is restricted to between -3 and -1.5 V in the figure to better illustrate the potential on the conductive surface. In Panel a the presence of the interconnects can be seen on the front of the solar panels by the light and dark patches, and the cut-off line at the bottom of the solar panel. The front of the solar panel also gains a slightly more positive potential and shows the same pattern as previously described from the motional electric field. However, the overall impact on the surface charging of the spacecraft body was found to be limited with a change of around 0.1 V measured with the currents from the interconnects only providing a small contribution to the overall current balance. This result illustrates that the presence of the interconnects does not provide any meaningful contribution to the surface charging in the plasmasphere, so will not account for any difference in simulation and data results. During the later stages of the JUICE mission it will explore the ionospheres of Jupiter's moons. These share a similar composition to the Earths plasmasphere, and so this result is an important indication that data obtained here will not be significantly impacted by the presence of the interconnects on the JUICE solar array.

https://doi.org/10.5194/egusphere-2026-2068
Preprint. Discussion started: 21 April 2026

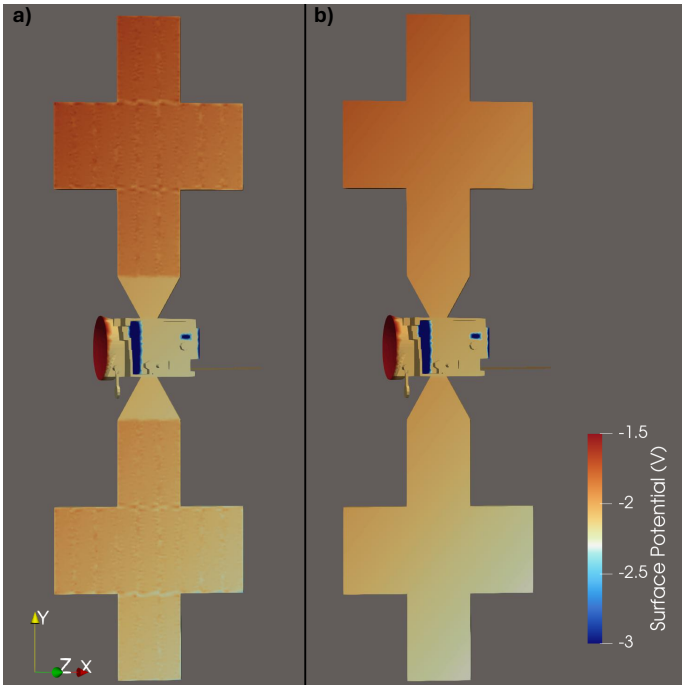

Figure 12. Diagram showing the potential obtained by the JUICE spacecraft with the potential range restricted to between -1.5 and -3 V. a) The potential of JUICE at closest approach with the addition of the interconnects on the front of the solar panel. b) The potential at closest approach without the addition of the interconnects on the solar panel for comparison.

5 Conclusions

The Earth swing-by allowed for the collection of data across the magnetosphere and magnetosheath, allowing for comparison and testing of the JUICE spacecraft in a relatively well understood environment in preparation for continuing mission to Jupiter and its icy moons. The results of the SPIS simulations conducted in the plasmasphere and magnetosheath provide an important step towards performing future correction techniques enhancing the data output. The effect of the different materials on the surface charging was shown through these simulations, highlighting how the dielectric surfaces could charge to significant negative potentials particularly in the magnetosheath. This will influence the measurements of nearby instruments such as the Langmuir probes. The behaviour of the different local particle populations was also illustrated due to the motion and potential of the spacecraft.

For the magnetosheath environment at 04:30 the SPIS simulations indicated an overall small positive charge of 2.5 V on the conductive surface of the spacecraft, with the positive charge primarily due to the emission of photoelectrons in this environment. The JEI instrument also indicates a small positive potential in the early magnetosheath, at around 03:00 a potential of around 5 V from the electron spectrum. This value is a rough initial estimate based on the lower cut-off of the photoelectrons. From the simulation in the early magnetosheath at 03:30 the average spacecraft potential here was 3.5 V. The simulated

https://doi.org/10.5194/egusphere-2026-2068
Preprint. Discussion started: 21 April 2026

potential is similar to the value observed for the magnetosheath, taking into account as well that these measurements are for slightly different locations and that 5 V is an initial estimate for the potential here.

The dielectric surfaces charge to potentials from 7 to -70 V, depending on their position on the spacecraft. These potentials will impact measurements from the JDC, JEI and Langmuir probes, particularly for measurements made of the cold plasma population. A formation of an ion wake was also seen here, located around the JDC instrument. This will result in ion measurements made by JDC being underestimated, which may be corrected using further SPIS simulations. A photoelectron cloud was also observed, extending to the back of the spacecraft due to its positive potential. This background of photoelectrons is observed in the JEI measurements made and can make the observation of low energy electrons difficult.

During the closest approach from Earth in the plasmasphere, an overall negative charge of -2 V was found for the conductive surface, with potentials ranging from -0.8 to -6 V on the dielectric surfaces. In this cold and dense environment, negative charging is observed as the potential gained from the collected electrons dominates. The influence of positively biased potentials on the solar array was also explored but found to have no significant effect on the overall charging. This result will be important when exploring similar environments in the ionospheres of Jupiter's moons. The magnetic field is influential in this region affecting the shape of the photoelectrons emitted and resulting in a slight difference between the solar panel potentials due to these photoelectrons. A small ion wake was observed here as well as a depletion around the spacecraft. The presence of the ion wake and photoelectron cloud will again obscure low energy electron data and may result in an underestimation of JDC data.

The 2024 Earth-flyby allowed for an opportunity to begin preparation for the mission at Jupiter by testing the measurements made in the near Earth environment. Where similar environments will be encountered at Jupiter, this study provides a preliminary understanding of the surface charging and particle behaviours there. Future Earth flybys are also planned for the JUICE spacecraft in 2026 and 2029, where results from this study can again be applied. This study therefore lays the foundations required to apply future data corrections to the results obtained by JUICE.

Author contributions. Simulations were run and analysed by Maryam Zeroual and Mika Holmberg. Other co-authors supervise different JUICE instruments and support the analysis.

Competing interests. The authors declare no competing interests

Acknowledgements. This publication has emanated from research conducted with the financial support of Taighde Éireann - Research Ireland under Grant number [22/PATH-S/10757], awarded to MKGH.

We would like to acknowledge correspondence with Xuanye Ma in obtaining data from the SAMU dataset which was made possible with help from Dr. Katariina Nykyri. The code was originally developed by Andrew Dimmock.

The spacecraft model used for the simulations was adapted from a model originally developed by Christian Imhof at Airbus Defence and Space GmbH.

https://doi.org/10.5194/egusphere-2026-2068
Preprint. Discussion started: 21 April 2026

ARF's work at DIAS was supported by Taighde Éireann - Research Ireland Laureate Consolidator award SOLMEX

Work at LPC2E and Lagrange is co-funded by CNES.

Simulation results have been provided by the Community Coordinated Modeling Center (CCMC) at Goddard Space Flight Center through their publicly available simulation services (https://ccmc.gsfc.nasa.gov). The Open GGCM Model was developed by Joachim Raeder at the University of New Hampshire. This work was carried out using the SWMF and BATS-R-US tools developed at the University of Michigan's Center for Space Environment Modeling (CSEM). The modeling tools described in this publication are available online through the University of Michigan for download and are available for use at the Community Coordinated Modeling Center (CCMC).

https://doi.org/10.5194/egusphere-2026-2068
Preprint. Discussion started: 21 April 2026

References

Abe, T., Balan, N., Oyama, K.-I., and Bailey, G.: Plasmasphere electron temperature — Observations and theory, Advances in Space Research, 20, 401–405, https://doi.org/https://doi.org/10.1016/S0273-1177(97)00700-X, the Subauroral Ionosphere, Plasmasphere, Ring Current and Inner Magnetosphere System, 1997.

Balan, N., Oyama, K. I., Bailey, G. J., and Abe, T.: Plasmasphere electron temperature studies using satellite observations and a theoretical model, Journal of Geophysical Research: Space Physics, 101, 15 323–15 330, https://doi.org/https://doi.org/10.1029/96JA00823, 1996.

Bergman, S., Stenberg Wieser, G., Wieser, M., Johansson, F. L., and Eriksson, A.: The Influence of Varying Spacecraft Potentials and Debye Lengths on In Situ Low-Energy Ion Measurements, Journal of Geophysical Research: Space Physics, 125, e2020JA027 870, https://doi.org/https://doi.org/10.1029/2020JA027870, e2020JA027870 2020JA027870, 2020.

Bergman, S., Miyake, Y., Kasahara, S., Johansson, F. L., and Henri, P.: Spacecraft Charging Simulations of Probe B1 of Comet Interceptor during the Cometary Flyby, The Astrophysical Journal, 959, 138, https://doi.org/10.3847/1538-4357/ad0ce5, 2023.

Bochet, M., Bergman, S., Holmberg, M. K. G., Wieser, M., Wieser, G. S., Wittmann, P., Gourinat, Y., Imhof, C., and Barabash, S.: Perturbations of JUICE/JDC Ion Measurements Caused by Spacecraft Charging in the Jovian Magnetosphere and the Ionosphere of Ganymede, Journal of Geophysical Research: Space Physics, 128, e2023JA031 377, https://doi.org/https://doi.org/10.1029/2023JA031377, e2023JA031377 2023JA031377, 2023.

Boutonnet, A., Langevin, Y., and Erd, C.: Designing the JUICE Trajectory, Space Science Reviews, 220, 67, https://doi.org/10.1007/s11214-024-01093-y, 2024.

Carpenter, D. L. and Anderson, R. R.: An ISEE/whistler model of equatorial electron density in the magnetosphere, Journal of Geophysical Research: Space Physics, 97, 1097–1108, https://doi.org/https://doi.org/10.1029/91JA01548, 1992.

Chao, J., Wu, D., Lin, C.-H., Yang, Y.-H., Wang, X., Kessel, M., Chen, S., and Lepping, R.: Models for the size and shape of the earth's magnetopause and bow shock, in: Space Weather Study Using Multipoint Techniques, edited by Lyu, L.-H., vol. 12 of *COSPAR Colloquia Series*, pp. 127–135, Pergamon, https://doi.org/https://doi.org/10.1016/S0964-2749(02)80212-8, 2002.

Comfort, R.: Thermal structure of the plasmasphere, Advances in Space Research, 17, 175–184, https://doi.org/https://doi.org/10.1016/0273-1177(95)00710-V, 1996.

Craven, P. D., Comfort, R. H., Gallagher, D. L., and West, R.: A Study of the Statistical Behavior of Ion Temperatures from De 1 / RIMS, pp. 173–182, American Geophysical Union (AGU), ISBN 9781118663905, https://doi.org/https://doi.org/10.1029/GM062p0173, 1991.

Engwall, E., Eriksson, A. I., and Forest, J.: Wake formation behind positively charged spacecraft in flowing tenuous plasmas, Physics of Plasmas, 13, 062 904, https://doi.org/10.1063/1.2199207, 2006.

Fränz, M., Fischer, H., Krupp, N., Roussos, E., Wittmann, P., Bambach, P., Wahlund, J.-E., Stenberg Wieser, G., Barabash, S., Holmberg, M., Zeroual, M., Brandt, P. C., Wurz, P., Wieser, M., Futaana, Y., Shimoyama, M., Pontoni, A., Vorburger, A., Galli, A., Riedo, A., Ho, G., Mitchell, D. G., Clark, G., Kollmann, P., Gkioulidou, M., Regoli, L., Wimmer-Schweingruber, R., Asamura, K., Kallio, E., Opitz, A., Grande, M., Coates, A., Jones, G., McKenna-Lawlor, S., Sarris, T., Fedorov, A., André, N., and Baláž, J.: Ion composition of the Earth plasmasphere observed by the PEP-JEI and RPWI instruments on the JUICE satellite, Annales Geophysicae, in press, 2026.

Garrett, H. B.: The charging of spacecraft surfaces, Reviews of Geophysics, 19, 577–616, https://doi.org/https://doi.org/10.1029/RG019i004p00577, 1981.

https://doi.org/10.5194/egusphere-2026-2068
Preprint. Discussion started: 21 April 2026

Goldstein, J., Gallagher, D., Craven, P. D., Comfort, R. H., Genestreti, K. J., Mouikis, C., Spence, H., Kurth, W., Wygant, J., Skoug, R. M., Larsen, B. A., D. Reeves, G., and De Pascuale, S.: Temperature Dependence of Plasmaspheric Ion Composition, Journal of Geophysical Research: Space Physics, 124, 6585–6595, https://doi.org/https://doi.org/10.1029/2019JA026822, 2019.

Grasset, O., Dougherty, M., Coustenis, A., Bunce, E., Erd, C., Titov, D., Blanc, M., Coates, A., Drossart, P., Fletcher, L., Hussmann, H., Jaumann, R., Krupp, N., Lebreton, J.-P., Prieto-Ballesteros, O., Tortora, P., Tosi, F., and Van Hoolst, T.: JUpiter ICy moons Explorer (JUICE): An ESA mission to orbit Ganymede and to characterise the Jupiter system, Planetary and Space Science, 78, 1–21, https://doi.org/https://doi.org/10.1016/j.pss.2012.12.002, 2013.

Holmberg, M. K. G., Jackman, C. M., Taylor, M. G. G. T., Witasse, O., Wahlund, J.-E., Barabash, S., Michotte de Welle, B., Huybrighs, H. L. F., Imhof, C., Cipriani, F., Déprez, G., and Altobelli, N.: Surface Charging of the Jupiter Icy Moons Explorer (JUICE) Spacecraft in the Solar Wind at 1 AU, Journal of Geophysical Research: Space Physics, 129, e2023JA032 137, https://doi.org/https://doi.org/10.1029/2023JA032137, e2023JA032137 2023JA032137, 2024.

Johansson, F. L., Eriksson, A. I., Gilet, N., Henri, P., Wattieaux, G., Taylor, M. G. G. T., Imhof, C., and Cipriani, F.: A charging model for the Rosetta spacecraft, AA, 642, A43, https://doi.org/10.1051/0004-6361/202038592, 2020.

Kutiev, I., Oyama, K., and Abe, T.: Analytical representation of the plasmasphere electron temperature distribution based on Akebono data, Journal of Geophysical Research: Space Physics, 107, SMP 24–1–SMP 24–11, https://doi.org/https://doi.org/10.1029/2002JA009494, 2002.

Lemaire, J. F. and Gringauz, K. I.: The Earth's Plasmasphere, 1998.

Ma, X., Nykyri, K., Dimmock, A., and Chu, C.: Statistical Study of Solar Wind, Magnetosheath, and Magnetotail Plasma and Field Properties: 12+ Years of THEMIS Observations and MHD Simulations, Journal of Geophysical Research: Space Physics, 125, e2020JA028 209, https://doi.org/https://doi.org/10.1029/2020JA028209, e2020JA028209 10.1029/2020JA028209, 2020.

Maldonado, C. A., Resendiz Lira, P. A., Delzanno, G. L., Larsen, B. A., Reisenfeld, D. B., and Coffey, V.: A review of instrument techniques to measure magnetospheric cold electrons and ions, Frontiers in Astronomy and Space Sciences, Volume 9 - 2022, https://doi.org/10.3389/fspas.2022.1005845, 2023.

Michelagnoli, M., Focardi, M., Pudney, M., Renouf, I., Merola, P., Noce, V., Nunez, M. V., Dinuzzi, G., and Chiarucci, S.: Surface Charging Analysis of Ariel Spacecraft in L2-Relevant Space Plasma Environment and GEO Early Transfer Orbit, Aerospace, 11, https://doi.org/10.3390/aerospace11120988, 2024.

Minow, J. I., Jordanova, V. K., Pitchford, D., Ganushkina, N. Y., Zheng, Y., Luca Delzanno, G., Jun, I., and Kim, W.: ISWAT spacecraft surface charging review, Advances in Space Research, https://doi.org/https://doi.org/10.1016/j.asr.2024.08.058, 2024.

Ozhogin, P., Song, P., Tu, J., and Reinisch, B. W.: Evaluating the diffusive equilibrium models: Comparison with the IMAGE RPI field-aligned electron density measurements, Journal of Geophysical Research: Space Physics, 119, 4400–4411, https://doi.org/https://doi.org/10.1002/2014JA019982, 2014.

Rasinskaite, D., Watt, C. E. J., Forsyth, C., Smith, A. W., Lao, C. J., Chakraborty, S., Holmes, J. C., and Delzanno, G. L.: Estimating Electron Temperature and Density Using Van Allen Probe Data: Typical Behavior of Energetic Electrons in the Inner Magnetosphere, Journal of Geophysical Research: Space Physics, 130, e2024JA033 443, https://doi.org/https://doi.org/10.1029/2024JA033443, e2024JA033443 2024JA033443, 2025.

Ripoll, J.-F., Thaller, S. A., Hartley, D. P., Malaspina, D. M., Kurth, W. S., Cunningham, G. S., Pierrard, V., and Wygant, J.: Statistics and Models of the Electron Plasma Density From the Van Allen Probes, Journal of Geophysical Research: Space Physics, 129, e2024JA032 528, https://doi.org/https://doi.org/10.1029/2024JA032528, e2024JA032528 2024JA032528, 2024.

https://doi.org/10.5194/egusphere-2026-2068
Preprint. Discussion started: 21 April 2026

Sandel, B. R., Goldstein, J., Gallagher, D. L., and Spasojevic, M.: Extreme Ultraviolet Imager Observations of the Structure and Dynamics of the Plasmasphere, Space Science Reviews, 109, 25–46, https://doi.org/10.1023/B:SPAC.0000007511.47727.5b, 2003.

Sarrailh, P., Matéo-Vélez, J.-C., Hess, S. L. G., Roussel, J.-F., Thiébault, B., Forest, J., Jeanty-Ruard, B., Hilgers, A., Rodgers, D., Cipriani, F., and Payan, D.: SPIS 5: New Modeling Capabilities and Methods for Scientific Missions, IEEE Transactions on Plasma Science, 43, 2789–2798, https://doi.org/10.1109/TPS.2015.2445384, 2015.

Shue, J.-H., Song, P., Russell, C. T., Steinberg, J. T., Chao, J. K., Zastenker, G., Vaisberg, O. L., Kokubun, S., Singer, H. J., Detman, T. R., and Kawano, H.: Magnetopause location under extreme solar wind conditions, Journal of Geophysical Research: Space Physics, 103, 17 691–17 700, https://doi.org/https://doi.org/10.1029/98JA01103, 1998.

Singh, R., Singh, A. K., and Singh, D.: Plasmaspheric parameters as determined from whistler spectrograms: a review, Journal of Atmospheric and Solar-Terrestrial Physics, 60, 495–508, https://doi.org/https://doi.org/10.1016/S1364-6826(98)00001-7, 1998.

Tian, S., Frissell, N., w2ruf, Lewis, J., and Lei Cai, P.: tsssss/geopack: v1.0.12, https://doi.org/10.5281/zenodo.15110787, 2025.

Verigin, M., Kotova, G., Slavin, J., Szabo, A., Kessel, M., Safrankova, J., Nemecek, Z., Gombosi, T., Kabin, K., Shugaev, F., and Kalinchenko, A.: Analysis of the 3-D shape of the terrestrial bow shock by interball/magion 4 observations, Advances in Space Research, 28, 857–862, https://doi.org/https://doi.org/10.1016/S0273-1177(01)00502-6, 2001.

Wahlund, J.-E., Bergman, J. E. S., Åhlén, L., Puccio, W., Cecconi, B., Kasaba, Y., Müller-Wodarg, I., Rothkaehl, H., Morawski, M., Santolik, O., Soucek, J., Grygorczuk, J., Wisniewski, Ł., Henri, P., Rauch, J. L., Le Duff, O., Retinò, A., Mansour, M., Stverak, S., Laifr, J., Andrews, D., André, M., Benko, I., Berglund, M., Cripps, V., Cully, C., Davidsson, J., Dimmock, A., Edberg, N. J. T., Eriksson, A. I., Fredriksson, J., Gill, R., Gomis, S., Holback, B., Jansson, S.-E., Johansson, F., Johansson, E. P. G., Khotyaintsev, Y., Mårtensson, B., Morooka, M. W., Nilsson, T., Ohlsson, D., Pelikan, D., Richard, L., Shiwa, F., Vigren, E., Wong, H. C., Bonnin, X., Girard, J. N., Grosset, L., Henry, F., Lamy, L., Lebreton, J.-P., Zarka, P., Katoh, Y., Kita, H., Kumamoto, A., Misawa, H., Tsuchiya, F., Galand, M., Barcinski, T., Baran, J., Kowalski, T., Szewczyk, P., Grison, B., Jansky, J., Kolmasova, I., Lan, R., Pisa, D., Taubenschuss, U., Uhlir, L., Bochra, K., Borys, M., Duda, M., Kucinski, T., Ossowski, M., Palma, P., Tokarz, M., Colin, F., Dazzi, P., De Léon, E., Hachemi, T., Millet, A.-L., Randrianboarisson, O., Sene, O., Chust, T., Le Contel, O., Canu, P., Hadid, L., Sahraoui, F., Zouganelis, Y., Alison, D., Ba, N., Jeandet, A., Lebassard, M., Techer, J.-D., Mehrez, F., Varizat, L., Sumant, A. V., Sou, G., Hellinger, P., Travnicek, P., Bylander, L., Giono, G., Ivchenko, N., Kullen, A., Roth, L., Vaivads, A., Tanimoto, K., Mizuno, H., Sawamura, A., Suzuki, T., Namiki, M., Fujishima, S., Asai, K., Shimoyama, T., Fujii, M., Sato, Y., Birch, J., Bakhit, B., Greczynski, G., Gare, P., Landström, S., LeLetty, R., Ryszawa, E., Torralba, I., Trescastro, J. L., Osipenco, S., Wiklund, U., Roos, A., Söderström, J. C., Björneholm, O., Fischer, G., Nyberg, T., Kovi, K. K., Balikhin, M., Yearby, K. H., Holmberg, M., Jackman, C. M., Louis, C. K., Rhouni, A., Leray, V., Geyskens, N., Berthod, C., Lemaire, B., Clémencon, A., Wattieaux, G., André, N., Garnier, P., Génot, V., Louarn, P., Marchaudon, A., Modolo, R., Baskevitch, C.-A., Hess, L. G., Leclercq, L., Saur, J., Kimura, T., Kojima, H., Yagitani, S., and Miyoshi, Y.: The Radio & Plasma Wave Investigation (RPWI) for the JUpiter ICy moons Explorer (JUICE), Space Science Reviews, 221, 1, https://doi.org/10.1007/s11214-024-01110-0, 2024.

Whipple, E. C.: Potentials of surfaces in space, Reports on Progress in Physics, 44, 1197, https://doi.org/10.1088/0034-4885/44/11/002, 1981.

Zhang, Z., Liu, W., Zhang, D., and Cao, J.: Estimating the corotation lag of the plasmasphere based on the electric field measurements of the Van Allen Probes, Advances in Space Research, 73, 758–766, https://doi.org/https://doi.org/10.1016/j.asr.2023.10.022, 2024.